Mass spectrometric identification of in vitro-generated metabolites of two emerging organophosphate flame retardants : V6 and BDP

Accepted Manuscript

Mass spectrometric identification of *in vitro*-generated metabolites of two emerging organophosphate flame retardants: V6 and BDP

Andreia Alves, Claudio Erratico, Luisa Lucattini, Matthias Cuykx, Ana Ballesteros-Gómez, Pim E.G. Leonards, Stefan Voorspoels, Adrian Covaci

PII: S0045-6535(18)31617-5

DOI: 10.1016/j.chemosphere.2018.08.142

Reference: CHEM 22060

To appear in: *ECSN*

Received Date: 18 June 2018

Revised Date: 19 August 2018

Accepted Date: 28 August 2018

Please cite this article as: Alves, A., Erratico, C., Lucattini, L., Cuykx, M., Ballesteros-Gómez, A., Leonards, P.E.G., Voorspoels, S., Covaci, A., Mass spectrometric identification of *in vitro*-generated metabolites of two emerging organophosphate flame retardants: V6 and BDP, *Chemosphere* (2018), doi: 10.1016/j.chemosphere.2018.08.142.

Mass spectrometric identification of *in vitro*-generated metabolites of two emerging organophosphate flame retardants: V6 and BDP

Andreia Alves[a,$], Claudio Erratico[b,$], Luisa Lucattini[c], Matthias Cuykx[b], Ana Ballesteros-Gómez[c,d], Pim E.G. Leonards[c], Stefan Voorspoels[a], Adrian Covaci[b*]

[a] Flemish Institute for Technological Research (VITO NV), Boeretang 200, 2400 Mol, Belgium

[b] Toxicological Centre, Department of Pharmaceutical Sciences, University of Antwerp, Universiteitsplein 1, B-2610 Wilrijk, Belgium

[c] Department of Environment and Health, Vrije Universiteit Amsterdam, De Boelelaan 1087, 1081 HV Amsterdam, The Netherlands

[d] Department of Analytical Chemistry, Institute of Fine Chemistry and Nanochemistry, University of Córdoba, Marie Curie Building (Annex), Campus of Rabanales, 14071 Córdoba, Spain

$ - shared first authors: A. Alves and C. Erratico

*corresponding author: Adrian Covaci (University of Antwerp)

Email: adrian.covaci@uantwerpen.be

Abstract

The aim of the present study was to investigate the *in vitro* metabolism of two emerging organophosphate flame retardants, namely tetrekis(2-chlorethyl)dichloroisopentyldiphosphate (V6) and bisphenol-A bis-diphenyl phosphate (BDP) in human liver microsomes (HLMs), HLM S9 fractions and in human serum. In particular, the role of cytochrome P450 (CYPs) enzymes and/or paraoxonases (PONs) in the formation of V6 and BDP phase I metabolites was studied. Mono-, di-hydroxylated and hydrolytic phase I metabolites of V6 were mainly formed by CYPs in HLMs, while hydrolytic and O-dealkylated phase I metabolites of BDP were generated by PONs mainly in serum experiments. Limited number of glucuronidated and sulfated phase II metabolites were also identified for the two chemicals. The activity of seven recombinant CYPs (rCYPs) including rCYP1A2, rCYP2B6, rCYP2C9, rCYP2C19, rCYP2D6, rCYP2E1 and rCYP3A4 in the *in vitro* phase I metabolism of V6 and BDP was investigated. The formation of V6 metabolites was catalyzed by several enzymes, especially rCYP1A2 that was responsible for the exclusive formation of two metabolites, one primary (M1) and its secondary metabolite (M9). For BDP, only one phase I metabolite (MM1) was catalyzed by the seven rCYPs. Collectively, these results indicate that CYPs have a predominant role in the metabolism of V6, while PONs have a predominant role in BDP *in vitro* metabolism. These results are a starting point for future studies involving the study of the toxicity, bioaccumulation and *in vivo* biomonitoring of V6 and BDP.

Keywords: *In vitro* metabolism, V6, BDP, human liver fractions, recombinant CYPs, LC-QTOF-MS

1. Introduction

Alternative flame retardants (FRs) have been increasingly used in all variety of consumer goods, such as electronics, furniture, textiles and plastics after restrictions on the use of polybrominated diphenyl ethers (PBDEs) (Van Der Veen and de Boer, 2012). In 2006, among the "new" FRs, the phosphorous FRs (PFRs) already represented more than 20% of the total FR consumption in Europe. This percentage included 11 % of chlorinated PFRs and 9 % of non-halogenated FRs (Van Der Veen and de Boer, 2012).

2,2-Bis(chloromethyl) trimethylene bis[bis(2-chloroethyl) phosphate] or commonly named tetrekis(2-chlorethyl)-dichloroisopentyldiphosphate (V6) is an halogenated phosphate ester mainly used as additive FR. It is used in specific applications in combination with two other FRs, i.e. tris(1-chloro-isopropyl)phosphate (TCIPP) and tris(1,3-dichloro-2-propyl)phosphate (TDCPP), and only when their FR properties needed to be enhanced (EU, 2008; Van Der Veen and de Boer, 2012). V6 has been mainly used in polyurethane foam and applications have been reported in furniture, automotive and baby products (Stapleton et al., 2011; Fang et al., 2013). Data about the production market of V6 is scarce: about 454−4,500 tons in the USA in 1998 and unknown in China (Fang et al., 2013) and less than 5,000 tons in EU in 2000 (EU, 2008).

However, due to the risks related to its primary impurity, tris(2-chloroethyl)phosphate (TCEP) (4.5-7.5% (w/w)), V6 was suggested to be classified as Category 3 carcinogen R40 (limited evidence of carcinogenic effect) if the TCEP content exceeds 1.0% and category 2 for fertility, R60 (may impair fertility) above 0.5% TCEP (EU, 2008). Among various toxic effects, reproductive, developmental, birth defect, chromosome abnormalities are related to V6 (EU, 2008; Van Der Veen and de Boer, 2012).

Another chemical of interest in the present study is Bisphenol-A bis diphenyl phosphate (BDP, CAS 5945-33-5), an aryl phosphate ester used as one of the primary non-halogenated replacements for the Deca-BDE technical mixture. BDP is mainly used in electronics (Van Der Veen and de Boer, 2012; Ballesteros-Gomez et al., 2014), but also in flooring, textiles and

furniture (LCSP, 2005; ECHA, 2014). Its presence has been reported in polycarbonate/acrylonitrile butadiene styrene (PC/ABS) and high impact polystyrene/poly(2,6-dimethyl-1,4-phenylene oxide) (HIPS/PPO) plastics (LCSP, 2005). Nowadays, it is mainly used as a substitute for triphenyl phosphate (TPHP) due to its lower volatility (Pawlowski and Schartel, 2007). BDP represents around 85% of the mixture which results from the reaction of phosphoric trichloride with bisphenol A and phenol. The U.S. production/import volume for this mixture was reported as 4500-23,000 tons in 2006 (OEHHA, 2012; Krowech et al., 2016).

BDP showed low to moderate aquatic toxicity (EC50 > 1 mg/L, algae, growth inhibition) (Washington State 2006), while the NOEL for developmental effects on rats was high (1000 mg/kg/day) (Pakalin et al., 2007). Although, the *in vivo* toxicity to rats was described in several studies to be low, with a minimum median lethal dose (LD50) of 2000 mg/kg bw (EU, 2011), the BDP *in vivo* toxicity was classified as high for endocrine disrupting characteristics in humans due to its degradation product, bisphenol-A (NTP-CERHR, 2008).

There is a need for the human biomonitoring of emerging FRs (Van Der Veen and de Boer, 2012) due to many knowledge gaps in their toxicity and potential long term health effects and due to their estimated daily intake, which may be similar or even higher than those observed for polybrominated diphenyl ethers (PBDEs) (Dirtu et al., 2012; Christia et al., 2018). *In vitro* metabolism studies with human subcellular preparations have been reported before as a suitable strategy to elucidate the main human metabolic pathways and to identify suitable biomarkers for PFRs (Van den Eede et al., 2013, 2015, 2016). These studies showed a wide array of possible phase I and phase II metabolites of PFRs, resulting from mono- and di-hydroxylation, O-dealkylation, glucuronidation or sulfation (Van den Eede et al., 2013, 2015, 2016).

However, this was not yet done for exploring the metabolism of V6 and BDP *in vitro* and therefore the main goals of the present study comprised: 1) the identification of major phase I and phase II (glucuronide and/or sulfate conjugates) metabolites of V6 and BDP; 2) the understanding of main metabolic pathways involved in the formation of phase-I and phase-II

metabolites, including the identification of the responsible enzymes involved; 3) the identification of the role of nine recombinant human CYP enzymes (rCYPs) in the formation of the phase-I metabolites in HLM.

2. Experimental procedures

2.1 Chemicals and Reagents

Neat standards for BDP (purity >98%) and V6 (purity >98%) were obtained from TRC (Toronto, Canada) and from AccuStandard (Hattersheim, Germany), respectively. All standard stock solutions were prepared in methanol (1 mM). Theophylline (internal standard, IS), tramadol, chlorpyrifos-oxon (used as positive controls for CYPs and paraoxonases (PONs), respectively), 2,6-uridine-diphosphate glucuronic acid (UDPGA), tris(hydroxmethyl) aminomethane (TRIS), alamethicin, adenosine 3'-phosphate 5'-phosphosulfate (PAPS) (purity ≥60%), calcium chloride ($CaCl_2$) and NADPH-regenerating system (all neat, purity >99%) were obtained from Sigma-Aldrich (Diegem, Belgium).

Pooled human liver microsomes (HLMs; mix gender, n=200) were purchased from Tebu-bio (Boechout, Belgium). Serum was collected in the frame of an ongoing study (registered at http://clinicaltrials.gov/ with number NCT01778868). This study was approved by the Ethical Committee of the Antwerp University Hospital (Belgian Registry number B30020097009) and all participants provided their written informed consent. Serum from 10 adult lean volunteers (mix of females and males) was pooled and stored at -20°C until analysis.

Acetonitrile, methanol and formic acid (analytical grade) were obtained from Merck KgA Chemicals (Darmstadt, Germany) and ultrapure water (18.2 MΩ) from an Elga LabWater water purification instrument (Saint Maurice, France).

2.2 Strategy to characterize the *in vitro* metabolism of V6 and BDP

Firstly, *in vitro* metabolism studies were conducted for V6 and BDP using human liver microsomes (HLM) and S9 fractions and human serum. Also, the phase I metabolites generated were hypothesized to be further transformed by uridine diphosphate glucuronic acid transferase (UGT) enzymes and sulfotransferase (SULT) enzymes. A summary of the experiments carried out for the activation of each enzyme is given in Table 1.

2.2.1 CYPs-mediated metabolism assay

The reaction mixture contained phosphate buffer (pH adjusted to 7.4), HLM (0.5 mg/mL) and individual substrates (10 µM of V6 and BDP) on ice (final volume: 950 µL). After 5 min pre-incubation in a shaking water bath at 37 °C, the reaction was initiated by addition of 50 µL of NADPH-regenerating solution (1 mM final concentration). The reaction was stopped after 2 h by adding 700 µL of an ice-cold acetonitrile solution containing 1% formic acid (*v/v*) and 1.0 µg/mL of IS solution (final concentration of 0.4 µg/mL in the extract). The samples were vortexed for 30s and centrifuged at 3,500 g for 3 min. The supernatant (~1.1 mL) was transferred into a new vial containing 230 mg of NH_4Ac (to induce a salting-out separation of acetonitrile-water), vortexed for 30 s and centrifuged at 3,500 g for 2 min. Afterwards, a 500 µL aliquot of the supernatant was transferred into a new tube. The liquid-to-liquid extraction step was repeated two more times transferring 700 and 800 µL aliquots of the supernatant, respectively. The three extracts were pooled, blown down to dryness under gentle nitrogen flow at room temperature and resuspended in 100 µL of 70:30 H_2O:MeOH (*v/v*) for BDP experiments (or in 100 µL of 90:10 of H_2O:MeOH (*v/v*) solution for V6 experiments).

2.2.2 PON-mediated metabolism assay in HLM S9 fractions and serum

The reaction mixture contained individual substrates (10 µM) diluted in 0.1 M glycine-NaOH buffer (pH 10.0) containing calcium chloride (1 mM) and sodium chloride (0.3 M) in a volume of 450 µL containing the substrate (V6 or BDP, 10 µM). After 5-min pre-incubation in a shaking

water bath at 37°C, the reaction was initiated adding 50 µL of HLM S9 fraction (0.5 mg/mL, final concentration). The reaction was carried for a maximum of 3h, adding NADPH regenerating system to the incubation.

To investigate V6 and BDP metabolism mediated by serum PONs, the same reaction mixture was prepared and initiated by adding 10 µL of pooled human serum (n=10), instead of HLM S9 fractions. Samples were then processed as described in the above section.

2.2.3 UGT and SULT-mediated metabolism assay

For UGT-mediated metabolism, reaction mixtures were prepared as described above for CYP enzyme samples but adding a 10 µL aliquot of alamethicin (10 µg/mL) dissolved in dimethyl sulfoxide (<1% *v/v*) before pre-incubating the samples. The cofactors used were a NADPH-regenerating solution and UDPGA (1 mM, final concentration). For SULT-mediated metabolism, reaction mixtures were prepared as described above for CYP enzyme samples but using human liver S9 fraction (HLM S9; 0.5 mg/mL). The cofactors used were a NADPH-regenerating solution and PAPS (1 mM). Samples were then processed as described in the section 2.2.1 above.

2.2.4 Positive and Negative controls

Positive and negative control samples for each family of enzymes of interest were prepared as described above for phase I and phase II metabolism. Positive control samples were prepared using tramadol, chlorpyrifos-oxon and methylenedioxypyrovalerone (MDPV) as marker substrates for CYPs (Subrahmanyam et al., 2001), PONs (Davies et al., 1996) and UGTs and SULTs (Negreira et al., 2015), respectively. The formation of the corresponding marker metabolites was monitored (i.e for CYPs two primary metabolites resulted from the methylation of tramadol in the terminal NH_2 and in the OH substituted in the aromatic ring were monitored; for PONs there was a metabolite resulted from the hydrolysis of the P-O bond of chlorpyrifos-

oxon and in the phase II metabolism, the metabolites resulted from the conjugation reactions between MPDV and SULF or GLUC were used as positive controls).

Negative controls were prepared in each experiment in order to assure unequivocal determination of all metabolites. For CYPs-, UGTs- and SULT-mediated metabolism, three different negative control samples were prepared by replacing the enzymes (HLMs or HLS9 fraction), the substrate or the specific cofactor (NADPH, UDPGA or PAPS) in the reaction mixture with an equivalent aliquot of buffer, acetonitrile or buffer, respectively. For PON-mediated metabolism, only substrate and enzyme negative control samples (HLM for PONs) were prepared. To monitor chemical hydrolysis reaction and to determine the impurities eventually present in the stock solutions of the substrates, phosphate buffer (pH 7.4) or glycine buffer (pH 10) were used to dissolve individual standards (10 µM) and incubated alongside the metabolism samples. All positive and negative control samples were prepared according to the method described in the section 2.2.1.

2.2.5 Kinetics of the phase I metabolites

Kinetic experiments were conducted using HLM, varying the concentration of each substrate used (1 to 10 µM), the enzyme concentration (0.1-0.5 mg/mL, final concentration) and the incubation time (0 to 60 min). The samples were incubated and processed as described in the section 2.2.1.

2.2.6 Reaction phenotyping using human recombinant CYPs

The role of seven human recombinant CYP enzymes including rCYP1A2, rCYP2B6, rCYP2C9, rCYP2C19, rCYP2D6, rCYP2E1 and rCYP3A4 in the metabolism of V6 and BDP was investigated. Reaction mixtures were prepared as described in section 2.2.1, but using each human rCYP (20 pmol/mL, final concentration) instead of HLMs. The reaction was allowed to

proceed for 1h. Negative control samples were prepared by replacing the human rCYP with an equivalent aliquot of phosphate buffer.

2.3 LC-QTOF-MS analysis

The liquid chromatography-quadrupole-time-of-flight mass spectrometry (LC-QTOF-MS) system used consisted of a 1290 Infinity LC (Agilent Technologies, Santa Clara, California, USA) coupled to a 6530 Accurate-Mass QTOF-MS (Agilent Technologies, Santa Clara, California, USA). The chromatographic separation of V6 and BDP metabolites was performed using a XBridge C18 column (150 × 2.1 mm, 2.6 µm) from Waters (Milford, MA, USA) heated at 40°C. The mobile phases consisted of water (A) and methanol (B) both buffered with 0.1 % formic acid. For the separation of V6 and its metabolites, the following elution gradient was used: 0-2 min 10% B; 2-12 min 10-60% B, 12-27 min 60-90% B; 27-30min 90% B; 30-31 min 90-10% B; 31-36 min 90% B isocratic. For separation of BDP and its metabolites, the following elution gradient was used: 0-2 min 30% B; 2-15 min 30-70% B; 15-30 min 70-100% B; 30-35 min 100% B isocratic; 35-36 min 100-30% B; 36-40 min 30% B isocratic. The flow rate was 0.2 mL/min and the injection volume was 10 µL for both the methods.

The QTOF-MS was tuned and calibrated (mass accuracy within ±2 ppm) before each analysis using a solution containing reference masses (Agilent Technologies, Santa Clara, California, USA) up to 1,700 mass-to-charge ratio (*m/z*) using the extended dynamic range (2 GHz). Samples were analyzed using positive and negative electrospray ionization modes (ESI), with gas temperature at 300 ºC; gas flow at 10 mL/min; nebulizer pressure at 40 psi; sheath gas temperature at 250 ºC; sheath gas flow at 11 mL/min. Capillary and fragmentor voltages were set to 3,500 and 90 V, respectively. The QTOF-MS was set to acquire *m/z* ranging between 50 and 1,000 amu at a scan rate of 3 spectra per sec (0.33 ms/spectrum). The auto-MS/MS feature was used to obtain MS/MS spectra of precursor ions, using three different collision energy values

(10, 20 and 40 eV). During analysis, the mass accuracy of the QTOF (± 10 ppm) was constantly monitored by measuring reference masses ranging from *m/z* of 121 to 922 for both ESI modes.

2.4 Data analysis

Using a targeted approach, a list of predicted metabolites potentially formed in humans by the target families of enzymes was generated by Meteor Nexus software (v1.5, Lhasa Limited). Nexus is an expert knowledge-based software which gives predictions for a variety of toxicological endpoints. Meteor is the metabolic counterpart of Derek Nexus and can be used in conjunction with Derek to assess potential metabolites of compounds and their potential toxicity. Meteor uses a similar expert knowledge base system similar to Derek (based SAR program which contains expert rules (derived from public and proprietary data), but derived from metabolic data. The Meteor Nexus was used to predict the metabolites formed in vitro (phase 1 and phase 2) by several enzymes in HLM. As outcome of the prediction, the formula, structure, reaction involved, enzyme, log P, likelihood, parent and intermediate compounds could be generated. Then, the list of generated metabolites was imported (in the *.csv* format) in the Mass Hunter Qualitative analysis software (Agilent), in order to verify the presence of the molecular ion of a predicted metabolite of V6 or BDP. The precursor ions identified by MS mode were also fragmented in MS/MS mode using several collision induction dissociation (CID) energy values (10 to 40 eV) to confirm the structures on the basis of the major fragments. The presence of false positive peaks due to in-source fragmentation of other (related) compounds was investigated to prevent misidentification of compounds.

The main criteria for identification of metabolites were as follows: (a) peak signal-to-noise ratio (S/N) > 10, (b) the measured precursor *m/z* value should be within ±10 ppm of its predicted value; (c) lack of the precursor ion at the same retention time in all the negative control samples; (d) the isotope pattern should be identical to the predicted abundances; and (e) if the precursor *m/z* was fragmented, its fragmentation pattern should be explainable.

3. Results and Discussion

For the first time, *in vitro* phase-I and phase-II metabolism of V6 and BDP was investigated in humans. As CYPs, PONs, UGTs and SULTs were selected as the family of enzymes possibly involved in the V6 and BDP metabolism, positive controls for each of these families of enzymes were prepared as quality control (Table SI-1, Supporting Information). Lack of detection of any of these marker metabolites in the corresponding enzyme and substrate negative controls suggests that the preparations used were metabolically competent for the families of enzymes tested.

3.1 *In vitro* metabolites of V6 in HLM and S9 fraction

The structure, compound name, retention time, proposed chemical formula, predicted and measured *m/z* ratio and mass accuracy (measured in Δ ppm) of the V6 metabolites detected are presented in Table 2. Also, the expected and measured isotopic pattern of V6 and most of its *in vitro* metabolites are reported in Figure SI-1 (Supporting Information).

With very few exceptions (presented and discussed below), all identified V6 metabolites were not detected in any of the negative control samples prepared, did not result from in-source fragmentation of V6 or other V6 metabolites with higher m/z value and showed a retention time value not higher than that of V6 itself. Also, the measured isotopic patterns of the V6 metabolites detected matched the corresponding expected ones and in the vast majority of the cases the amount of each metabolite formed increased with increasing incubation time, protein and substrate concentrations (see Supporting Information, Figures SI-2 to SI-4). These results consistently suggest that the compounds detected are true V6 metabolites matching the proposed chemical formula.

A first pathway of V6 metabolism is the cleavage at one of the four outer and at one of the two inner oxygen atoms forming M1 and M2, respectively (Figure 1). As both M1 and M2 were

detected only in samples containing NADPH, our results suggest that they are formed only by CYPs. Also, looking at the structure of V6, it suggests that M1 and M2 were formed by *O*-dealkylation due to oxidation of the carbon atom next to one of the outer or of the inner oxygen atoms of V6, respectively. The structure of M1 was further elucidated using its MS/MS spectra (Figure SI-5, Supporting Information). Also, a peak corresponding to a metabolite resulting from hydrolysis of the P-O bond in the V6 structure ($[M+H]^+$ 378.9612 at 20.8 min) was also detected. However, the peak intensity was equal in samples with or without NADPH, suggesting that its formation is not catalyzed by CYPs. The same peak intensity was obtained in the enzyme (HLM) negative control sample, suggesting that no microsomal enzyme (including hydrolytic enzymes, like PONs and carboxylesterases) is needed for its formation. Last, the same peak was not detected neither in the V6 negative control sample, nor in the V6 stock solution, suggesting that V6 is needed for its formation and that the peak eluting at 20.8 min is not an eventual impurity of V6 stock solution. Collectively, these results suggest that the peak detected at 20.8 min ($[M+H]^+$ 378.9612) is only the result of chemical hydrolysis of V6 occurring in the phosphate buffer used and, therefore, it is not a true metabolite of V6, but it is instead a degradation product of V6.

M1 is further metabolized to a secondary metabolite (i.e M9) while no further secondary metabolite of M2 was detected. One chlorine atom of M1 is replaced by a hydroxylated group forming M9 (Figure 1). This reaction is known as oxidative dehalogenation which is preferentially catalyzed by CYP2E1 (Klaasens and Doull, 2007).

A second pathway of V6 metabolism is the direct addition of an oxygen atom (forming M3 and M4). Unfortunately, due to low abundances of M3 and M4, reliable MS/MS spectra could not be acquired, and therefore our data does not allow us to clarify where the newly formed hydroxylated groups are placed along the V6 molecule. However, considering the structure of V6, the carbon atoms where an oxygen atom can be added without causing *O*-dealkylation are the carbon atoms next to the terminal six chlorine atoms of V6. Also, these metabolites are further metabolized by oxidative dehalogenation forming M7 and M8 (Figure 1).

A third pathway of V6 metabolism is oxidative dechlorination (forming M5 and M6). The structure of M6 was confirmed using the fragments reported in its MS/MS spectra (Supporting Information, Figure SI-5). Then, M5 and M6 are further metabolized in three different ways. First, they form the corresponding carboxylic acids, although the intermediate aldehydes that are typically formed were not detected. Second, either M5 or M6 forms a sulfate conjugated (Figure 1). Third, either M5 or M6 undergoes oxidative dechlorination for a second time (forming M10), which in turn undergoes *O*-dealkylation (forming M11). Since these reactions are catalyzed by CYPs, our data suggest that the role of this family of enzymes in the oxidative metabolism of V6 *in vitro* is predominant.

3.2 *In vitro* metabolites of V6 produced by PONs

Formation of V6 metabolites by PONs was monitored in HLM and human serum. In serum incubations, two signals corresponding to M1 (but with a retention time of 20.7 instead of 22.0 min) and to a potential V6 metabolite ($[M+H]^+$ 378.9612 (M12) and retention time of 20.8 min) were detected. Both of these potential V6 metabolites can result from chemical and/or enzymatic (PONs-catalyzed) hydrolysis. However, the intensity of both these peaks was the same in the metabolism sample (containing buffer, human serum and V6) and in the enzyme negative control (i.e. without human serum), suggesting that their formation does not require enzymes present in the human serum. Also, none of these two potential V6 metabolites were detected in the V6 negative control sample, suggesting that V6 is needed for their formation. As none of these two potential V6 metabolites were detected in the V6 stock solution, they are not impurities of the V6 stock solution used for our *in vitro* metabolism incubations. Therefore, collectively our results consistently suggest that the two signals detected correspond to products of V6, possibly produced by chemical hydrolysis. Therefore, these two peaks were not considered as V6 metabolites. This conclusion is corroborated by the same findings obtained when using HLM incubations containing NADPH to assess the role of CYP enzymes in V6 metabolism.

3.3 Identification of the rCYPs involved in the metabolism of V6

Formation of five phase I metabolites was catalyzed in humans by the rCYPs (Figure 2). Two of them (i.e., the M1 and M9) are exclusively catalyzed by the same enzyme, the rCYP1A2 in which M1 is formed at higher levels than the M9. However, there are other enzymes such as rCYP2C9, rCYP2C19 and rCYP3A4 that catalyze the formation of another V6 metabolite, the M4, suggesting that its metabolism is not dependent of only one rCYP, as it happens in particular for M1 and M9. Also, M8 is catalyzed by two families of enzymes, the rCYP2C19 and rCYPs3A4 and M4 by rCYPC29 and rCYPC219. The formation of M12 is observed when the experiments were conducted in the presence of all individual rCYPs. Yet, this metabolite was detected in the enzyme negative control, therefore its formation is not exclusively dependent on the enzyme presence, suggesting that chemical hydrolysis was predominant in the formation of this metabolite in this assay and that none of the rCYPs was able to catalyze its formation (at least in detectable amounts). These results are again consistent with those obtained for HLM and HLM S9 fractions.

The V6 metabolites formed in higher amounts are M7, M8, M3 and M4. For instance, in further studies would be interesting to evaluate the dependence of formation of M7 and M8, once these are secondary metabolites of M3 & M4. Here, the rate and amounts formed of these two secondary metabolites could be conditioned by the amount of precursor molecules (M3 and M4), competition between compounds for the CYPs, substrate/incubation time/HLM. The evaluation of the formation of M3/M4 (after isolation) followed by the formation of M7/M8, could bring some insights about the selectivity in the V6 in vitro metabolism pathway and reactions involved by the CYPs (here the hydroxylation seems to have a predominant role).

3.4 *In vitro* metabolism of BDP

Six phase I metabolites of BDP were identified in incubations containing HLM without NADPH (Figure 3, Table 4). A first metabolite (MM1) was formed by the loss of diphenyl phosphate resulting from the hydrolysis of the corresponding P-O bond. As MM1 was also detected in enzyme negative control samples (about 20% of the signal in the metabolism sample), our data suggest that MM1 is mainly formed by enzymatic hydrolysis (possibly catalyzed by PONs) and by chemical hydrolysis. Two metabolites with the same pseudo-molecular ion (MM2 and MM3) were formed by the subsequent loss of a phenyl group of MM1. A tertiary metabolite (MM4) was subsequently formed by the loss of the phenyl group of MM2 or MM3. Since MM2, MM3, and MM4 were not detected in the enzyme or substrate negative control samples, our data suggest that chemical hydrolysis does not seem to be involved in their formation. Due to the low abundance of the pseudo-molecular ions of MM1-MM4, their isotopic pattern could not be measured. MS/MS spectra could only be obtained for MM1. It showed a characteristic fragment at *m/z* 135.08044 and formula $C_9H_{11}O$, corresponding to an isopropyl-phenol fragment.

As PONs are likely involved in the formation of MM1-MM4 and are expressed also in serum, the presence of MM1-MM4 was also screened in serum incubations. MM1 was detected with a twice as high signal intensity in the metabolism sample than in the enzyme negative control sample and not in the substrate negative control, suggesting that MM1 derives from BDP and that serum PONs are involved in its formation. In contrast, MM2 and MM3 were found at the same abundance in the metabolism sample and in the enzyme (serum) negative control sample but not in the substrate negative control sample. This suggests that MM2 and MM3 derive from BDP and that PONs present in serum are not involved in their formation as are those present in HLM.

Signals corresponding to a glucuronidated (MM1-Gluc) and a sulfated (MM1-Sulf) conjugate of MM1 were detected (Table 4) when HLMS9 fraction was incubated with BDP (MS/MS spectra in Supporting Information, Figure SI-6). The lack of detection of these compounds in

enzymes and co-factor (UDPGA and PAPS, respectively) negative controls suggests that these metabolites are true glucuronidated and sulfated conjugates of MM1 produced by UGTs and SULTs, respectively.

Two additional metabolites of BDP were also detected. Bisphenol-A (BPA) (MM6) was detected in serum incubations, but not in enzyme or substrate negative control samples (Table 4), suggesting that BPA is a true metabolite of BDP. BPA can be formed by hydrolysis of both the inner ether bonds of BDP, possibly catalyzed by serum PONs. As the intensity of BPA signal was low (approximately $1x10^3$), neither its isotopic pattern, nor its MS/MS spectra could be determined. Therefore, its identification is only tentative and remains to be confirmed.

The role of CYPs in BDP *in vitro* metabolism was also investigated. The only metabolite detected was the diphenylphosphate (MM5), not detected in NADPH, enzyme or substrate negative control samples. Diphenyl phosphate can result from *O*-dealkylation of the two inner oxygen atoms of BDP, in a similar way as seen for RDP (Ballesteros-Gomez et al., 2015). As the intensity of its signal was low (approximately $1x10^3$), neither its isotopic pattern, nor its MS/MS spectra were determined. Therefore, its identification remains to be confirmed. No other metabolite that can be formed by CYPs was detected.

3.5 Identification of the rCYPs involved in BDP metabolism

Incubating BDP with a panel of human rCYPs, only M1 could be detected (Figure 4). Although several human rCYPs were involved in its formation, our data suggest that rCYP3A4 was the most active rCYPs, followed by rCYP1A2 and rCYP2B6.

Previous studies have indicated that among several rCYPs, the CYP2B6 is effectively involved the *in vitro* metabolism of other FRs, such as BDE-99 (Erratico et al., 2012) or BDE-47 (Feo et al., 2013) and in the formation of their hydroxylated BDE metabolites in HLMs. Although, the activity of the rCYP2B6 in the phase I metabolism BDP and also for V6) was confirmed, it was not the predominant rCYP family involved in the metabolism of these FRs.

3.6 Human *in vitro* metabolism of BDP in comparison with other aryl-PFRs

Overall, our results suggest that PONs are a more active family of enzymes in the *in vitro* metabolism of BDP as compared to CYPs, which role seems to be almost negligible because of the very limited number of metabolites detected and their low relative amounts. This finding is in contrast with the largely predominant role of CYPs in the *in vitro* metabolism of TPHP (Van den Eede et al., 2013) and of resorcinol bis(diphenylphosphate) (RDP) in humans (Ballesteros-Gomez et al., 2015). As TPHP, RDP and BDP are arylphosphate flame retardants (PFRs), the results of the present study and those previously reported (Van den Eede et al., 2013) suggest that differences in chemical structures of individual PFRs can result in important differences in their *in vitro* (and possibly *in vivo*) metabolism.

The results reported in the present study underline the key importance of using the appropriate experimental design to be able to properly identify true *in vitro* metabolites of the substrate of interest and distinguish them from its chemical breakdown products, impurities eventually present in the standards used and from artifacts due to in-source fragmentation of the targets during analysis. The present study tentatively suggests new metabolites that can be suitable candidate biomarkers of human exposure of V6 and BDP in future biomonitoring studies.

Conflict of interest

The authors declare no conflict of interest.

Acknowledgements

Alves A., Lucattini L. and Erratico C. would like to acknowledge the FP7 project A-TEAM (*grant agreement* n° [316665]) by funding support of their PhD and Post-Doc grants (Marie Curie fellows). Ballesteros-Gomez A. acknowledges the funding by the Spanish Ministry of

Economy, Industry and Competitiveness (MINECO) for a Ramon y Cajal contract (RYC-2015-18482).

Supporting Information

The supporting Information to this article can be found in the online version. The quality control (IS detection) was performed for the experiments conducted with CYP, PONs, SULF and GLUC enzymes. MS isotopic pattern of the identified *in vitro* for V6 and BDP (phase I and phase II metabolites) is presented. MS/MS spectra and elucidation of the fragmentation of two phase I metabolites (M1 and M6) of V6 is disclosed. Time, substrate and HLM variation *vs*. response in the formation of V6 metabolites is presented.

References

Ballesteros-Gómez A., Brandsma S.H., de Boer J., Leonards P.E.G. (2014) Analysis of two alternative organophosphorus flame retardants in electronic and plastic consumer products: Resorcinol bis-(diphenylphosphate) (PBDPP) and bisphenol A bis (diphenyl phosphate) (BPA-BDPP). *Chemosphere 116*, 10–14.

Ballesteros-Gómez A., Van Den Eede N., Covaci A. (2015) In vitro human metabolism of the flame retardant resorcinol Bis(diphenylphosphate) (RDP). *Environ Sci Technol 49*, 3897–3904.

Christia C, Poma G, Besis A, Samara C, Covaci A (2018) Legacy and emerging organophosphorus flame retardants in car dust from Greece: Implications for human exposure. *Chemosphere* 196, 231-239.

Davies H.G., Richter R.J., Keifer M., et al. (1996) The effect of the human serum paraoxonase polymorphism is reversed with diazoxon, soman and sarin. *Nat Genet 14*, 334–336.

Dirtu A.C., Ali N., Van den Eede N., et al. (2012) Country specific comparison for the profiles of chlorinated, brominated and phosphate organic contaminants in indoor dust. Case study for Eastern Romania, 2010. *Environ Int 49*, 1–8.

ECHA (2014) Annex XV Restriction Report Proposal for a Restriction Substances name: Bis (pentabromophenyl) ether IUPAC name. European Chemicals Agency, Helsinki, Finland.

Erratico C., Szeitz A., Bandiera S.M. (2012) Oxidative metabolism of BDE-99 by human liver microsomes: predominant role of CYP2B6. *Toxicol Sci 129*, 280–92.

EU (2008) European Union Risk Assessment Report of 2,2-Bis(chloromethyl) trimethylene bis [bis(2-chloroethyl) Phosphate] (V6). Available at: https://echa.europa.eu/documents/ (https://echa.europa.eu/documents/10162/9e03b67c-8a0b-4de7-814e-a8a4ec63b9ae)

EU (2011) Discussion on "Hazardous Substances" Criterion Investigation of Request for Derogation. Available at: http://susproc.jrc.ec.europa.eu/imaging-equipment/docs/Ecolabel%20Criterion%20Derogations%20Hazardous%20Substances.pdf

Fang M., Webster T.F., Gooden D., et al. (2013) Investigating a novel flame retardant known as V6: Measurements in baby products, house dust, and car dust. *Environ Sci Technol 47*, 4449–4454.

Feo M.L., Gross M.S., Mcgarrigle B.P., et al. (2013) Biotransformation of BDE-47 to potentially toxic metabolites is predominantly mediated by human CYP2B6. *Environ Health Perspect 121*, 440–446.

Klaassen C. & Doull J. (2007) Casarett And Doull's Toxicology The Basic Science of Poisons. 7th Ed. Mcgraw-Hill Education – Europe.

Krowech G., Hoover S., Plummer L., Sandy M., et al. (2016) Identifying Chemical Groups for Biomonitoring. *Environ Health Perspect, 124*, A219-A226.

Lowell Center for Sustainable Production – LCSP (2005) Decabromodiphenylether : An Investigation of Non-Halogen Substitutes in Electronic Enclosure and Textile Applications. Available at: http://www.sustainableproduction.org/downloads/DecaBDESubstitutesFinal4-15-05.pdf

Negreira N., Erratico C., Kosjek T., et al. (2015) In vitro Phase I and Phase II metabolism of alpha-pyrrolidinovalerophenone (alpha-PVP), methylenedioxypyrovalerone (MDPV) and

methedrone by human liver microsomes and human liver cytosol. *Anal Bioanal Chem 407*, 5803–5816.

NTP-CERHR (2008). Monograph on the potential human reproductive and developmental effects of Bisphenol A. Available at: https://ntp.niehs.nih.gov/ntp/ohat/bisphenol/bisphenol.pdf

Office of Environmental Health Hazard Assessment (OEHHA, 2012). Non-halogenated Aromatic Phosphates. Materials for March 16, 2012 Meeting of Scientific Guidance Panel (SGP) Biomonitoring California. Available at: http://www.oehha.ca.gov/multimedia/biomon/pdf/031612NhArP.pdf

Pakalin S., Cole T., Steinkellner J, et al. (2007) Review on production processes of Decabromodiphenyl Ether (DecaBDE) used in polymeric applications in electrical and electronic equipment, and assessment of the availability of potential alternatives to Deca BDE. Eur Comm, document EUR 22693 EN (http://publications.jrc.ec.europa.eu/repository/handle/JRC36323).

Pawlowski K.H., Schartel B. (2007) Flame retardancy mechanisms of triphenyl phosphate, resorcinol bis(diphenyl phosphate) and bisphenol A bis(diphenyl phosphate) in polycarbonate/acrylonitrile–butadiene–styrene blends. *Polym Int 56*, 1404-1414.

Stapleton H.M., Klosterhaus S., Keller A., et al. (2011) Identification of flame retardants in polyurethane foam collected from baby products. *Environ Sci Technol 45*, 5323–5331.

Subrahmanyam V., Renwick A.B., Walters D.G., et al. (2001) Identification of cytochrome P-450 isoforms responsible for cis-tramadol metabolism in human liver microsomes. *Drug Metab Dispos 29*, 1146–1155.

Van den Eede N., Erratico C., Exarchou V., et al. (2015) In vitro biotransformation of tris(2-butoxyethyl) phosphate (TBOEP) in human liver and serum. *Toxicol Appl Pharmacol 284*, 246–253.

Van den Eede N., Maho W., Erratico C., et al. (2013) First insights into the metabolism of phosphate flame retardants and plasticizers using human liver fractions. *Toxicol Lett*, *223*, 9–15.

Van den Eede N., Tomy G., Tao F., et al. (2016) Kinetics of tris (1-chloro-2-propyl) phosphate (TCIPP) metabolism in human liver microsomes and serum. *Chemosphere 144*, 1299–1305.

Van Der Veen I., De Boer J. (2012) Phosphorus flame retardants: Properties, production, environmental occurrence, toxicity and analysis. *Chemosphere*, *88*, 1119–53.

Washington State Department of Ecology and Department of Health (2006) Washington State Polybrominated Diphenyl Ether (PBDE) Chemical Action Plan : Final Plan. Available at: https://fortress.wa.gov/ecy/publications/documents/0507048.pdf

495 **Table 1.** *In vitro* metabolism of V6 and BDP.

496

Enzyme	Fraction	Cofactor	Buffer	Metabolites	Reactions	Positive controls
CYPs	HLM	NADPH	Phosphate[a]	Phase I	Oxidation Hydrolysis	Tramadol
PONs	HLM, S9, serum	-	Tris-HCl[c]	Phase I	Hydrolysis	Chlorpyrifos-oxon
SULTs	S9	NADPH[b] + PAPs	Phosphate[a]	Phase II	Sulfation	MDPV[d]
UGTs	HLM	NADPH[b] + UDPGA	Phosphate[a]	Phase II	Glucuronidation	MDPV[d]

497 [a]100 mM phosphate buffer (pH 7.4); [b]NADPH Regenerating system; [c]100 µM Tris-HCl in 2 mM $CaCl_2$ (pH
498 8.0); [d] methylenedioxypyrovalerone

499

500 **Table 2.** Phase I and Phase II metabolites of V6 formed in *in vitro* in human liver
501 preparations (HLM and S9 fractions) and in human serum.

Structure	Compound (t_R, min)	Chemical formula	Molecular ion (m/z)		
			Target $[M+H]^+$	Measured $[M+H]^+$	Δ (ppm)
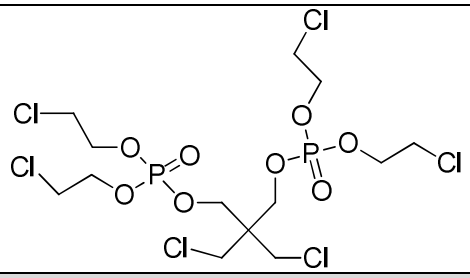	**V6** (24.9)	$C_{13}H_{24}Cl_6O_8P_2$	582.9122	582.9091	-5.32
Phase I metabolites					
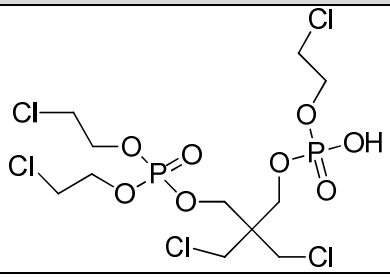	M1 (22.0)	$C_{11}H_{21}Cl_5O_8P_2$	520.9204	520.9198	1.15
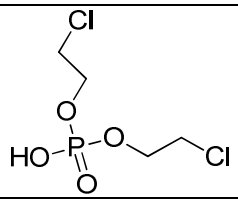	M2 (15.5)	$C_4H_9Cl_2O_4P$	222.9688	222.968	-3.59
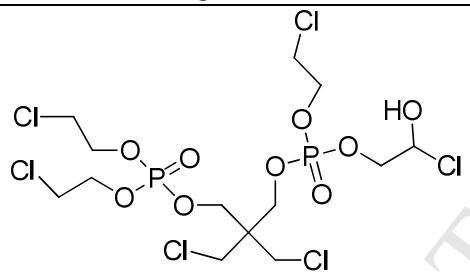	M3 (21.6)[a]	$C_{13}H_{24}Cl_6O_9P_2$	598.9071	598.9108	6.18
	M4 (22.8)[a]	$C_{13}H_{24}Cl_6O_9P_2$	598.9071	598.9067	-0.67
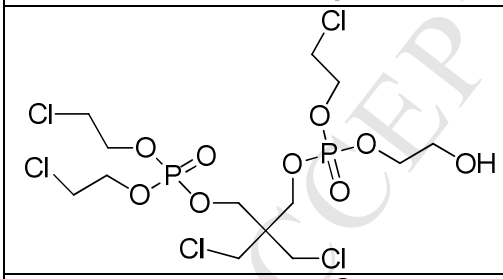	M5 (21.7)[a]	$C_{13}H_{25}Cl_5O_9P_2$	564.9461	564.9497	6.37
	M6 (22.1)[a]	$C_{13}H_{25}Cl_5O_9P_2$	564.9461	564.9470	1.59
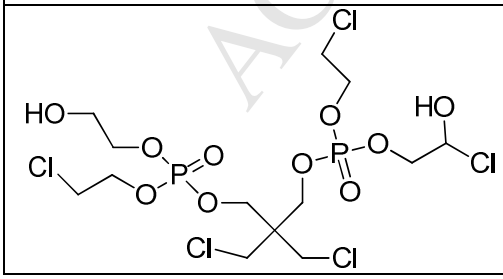	M7 (21.6)[a]	$C_{13}H_{25}Cl_5O_{10}P_2$	578.9254	578.9301	8.12
	M8 (22.8)[a]	$C_{13}H_{25}Cl_5O_{10}P_2$	578.9254	578.9239	-2.59

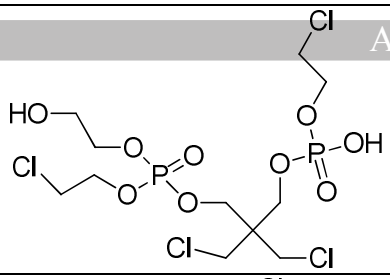	M9 (20.6)	$C_{11}H_{22}Cl_4O_9P_2$	502.9538	502.9582	8.75
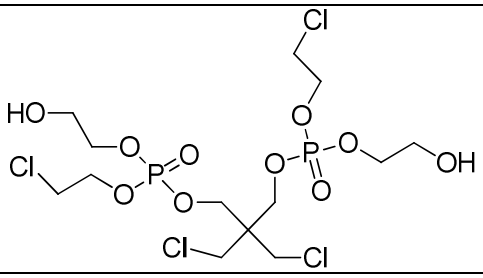	M10 (18.7)	$C_{13}H_{26}Cl_4O_{10}P_2$	546.9800	546.9807	1.28
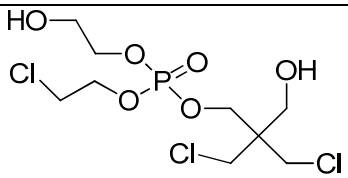	M11 (15.8)	$C_9H_{18}Cl_3O_6P$	358.9979	358.9998	5.29
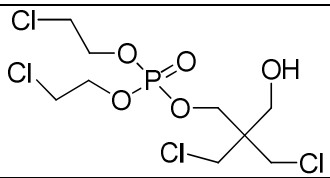	M12 (20.9)[b]	$C_9H_{17}Cl_4O_5P$	378.9612	378.9593	-5.01
Structure	**Compound (t_R, min)**	**Chemical formula**	**Molecular ion (m/z)**		
			Target $[M-H]^-$	**Measured $[M-H]^-$**	**Δ (ppm)**
Phase II metabolites					
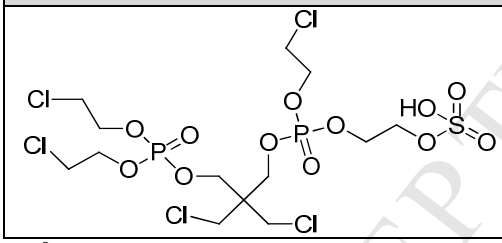	M5/M6-Sulf (23.1)	$C_{13}H_{25}Cl_5O_{12}P_2S_2$	642.8880	642.8884	-0.78

[a]Only one possible isomeric form is shown; [b] Mainly formed by chemical hydrolysis in the *in vitro* experiments

Table 3. Phase I and phase II metabolites of BDP formed in *in vitro* in human liver preparations (HLM and S9 fractions) and in human serum.

Structure	Compound (t_R, min)	Chemical formula	Molecular ion (m/z)		
			Target $[M+H]^+$	Measured $[M+H]^+$	Δ (ppm)
Phase I metabolites					
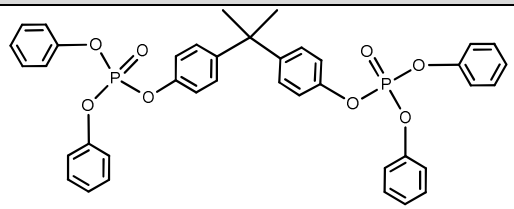	**BDP** (26.5)	$C_{39}H_{34}O_8P_2$	693.1802	694.1852	2.30
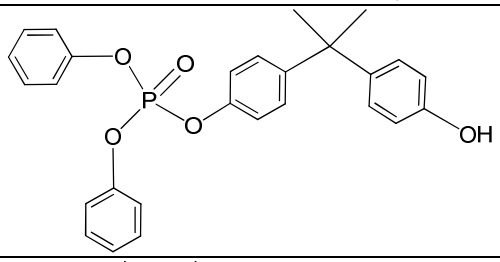	MM1 (22.0)	$C_{27}H_{25}O_5P$	461.1512	461.1529	3.69
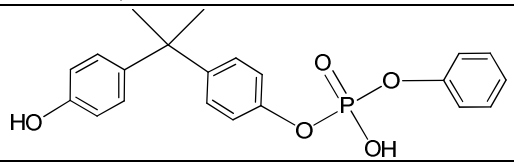	MM2 (9.06)	$C_{21}H_{21}O_5P$	385.1199	385.1161	-9.87
	MM3 (9.12)	$C_{21}H_{21}O_5P$	385.1199	385.1208	2.34
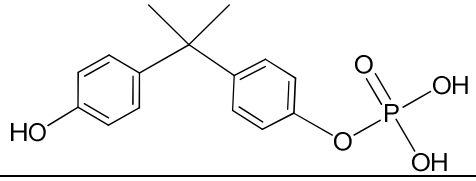	MM4 (12.2)	$C_{15}H_{17}O_5P$	309.0886	309.0882	-1.29
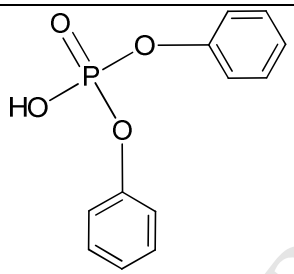	MM5 (20.1)	$C_{12}H_{11}O_4P$	251.0460	251.0468	3.19
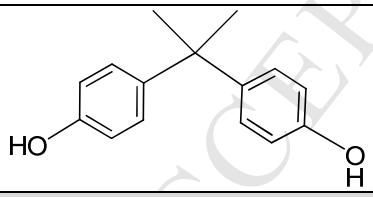	MM6 (18.3)	$C_{15}H_{16}O_2$	229.1223	229.1228	2.18
Phase II metabolites					
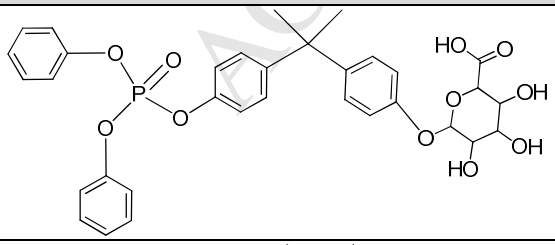	MM1-Gluc (20.0)	$C_{33}H_{33}O_{11}P$	635.1688	635.167	-2.83
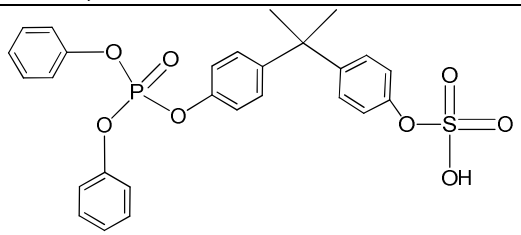	MM1-Sulf (23.1)	$C_{27}H_{25}O_8PS$	539.0935	539.0936	0.19

506 **Figure 1.** Scheme of V6 phase I and phase II metabolites formed in human liver fractions.

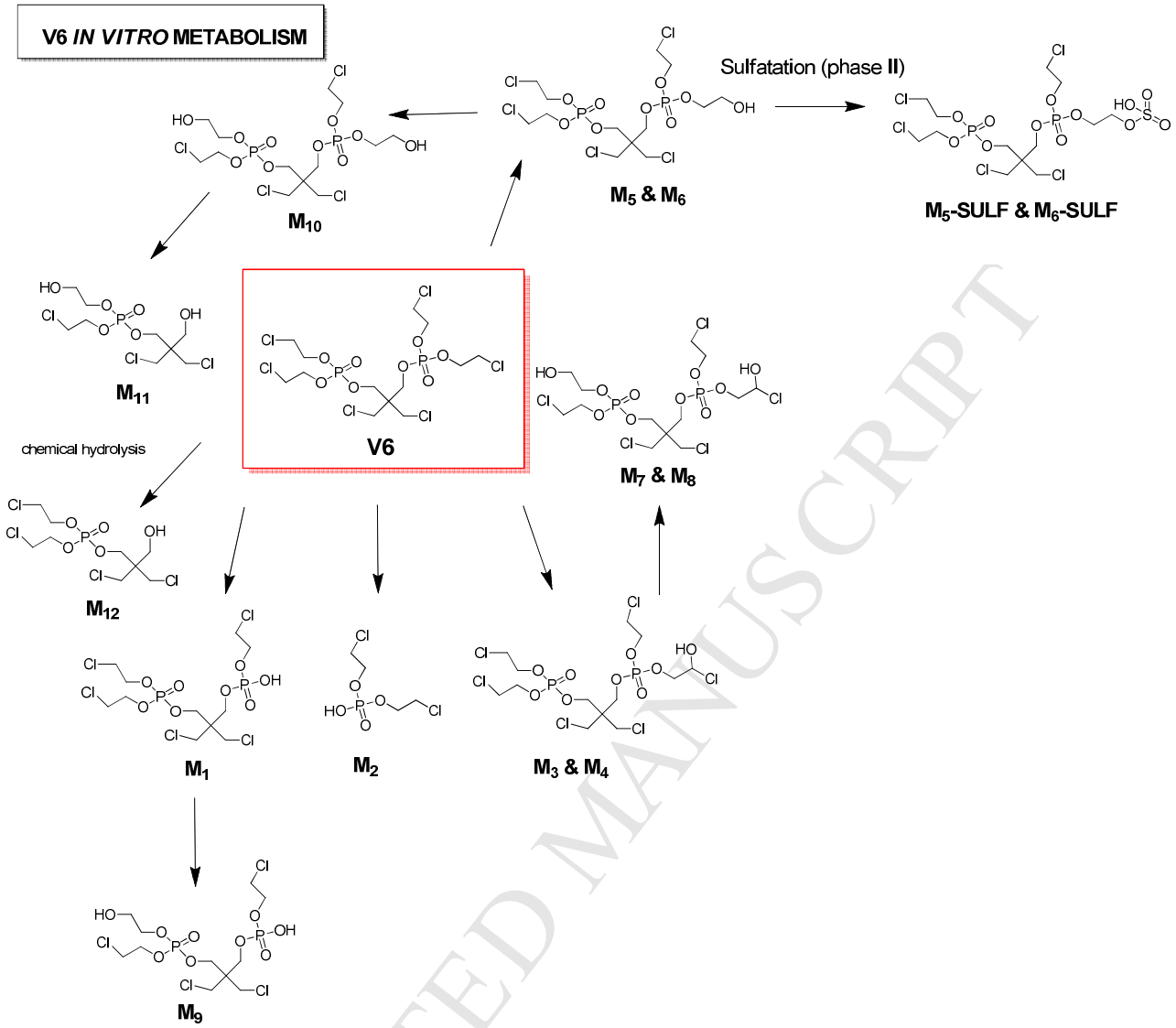

507

508

509 **Figure 2.** Formation of V6 phase I metabolites by seven rCYPs expressed in human liver.

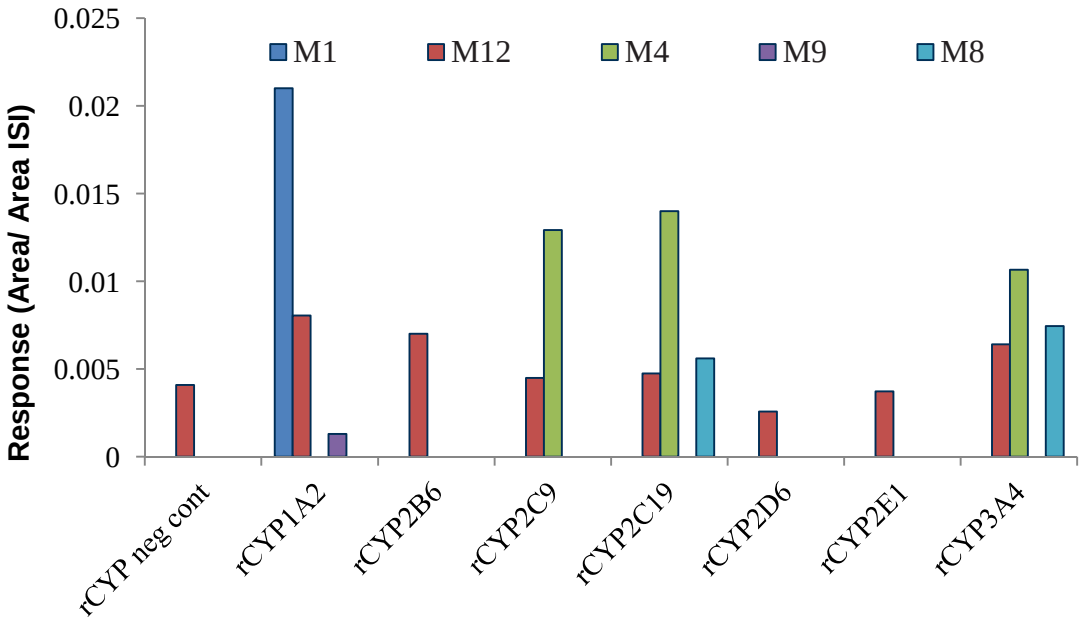

510

511

Figure 3. Scheme of BDP phase I and phase II metabolites formed by CYP and PON enzymes.

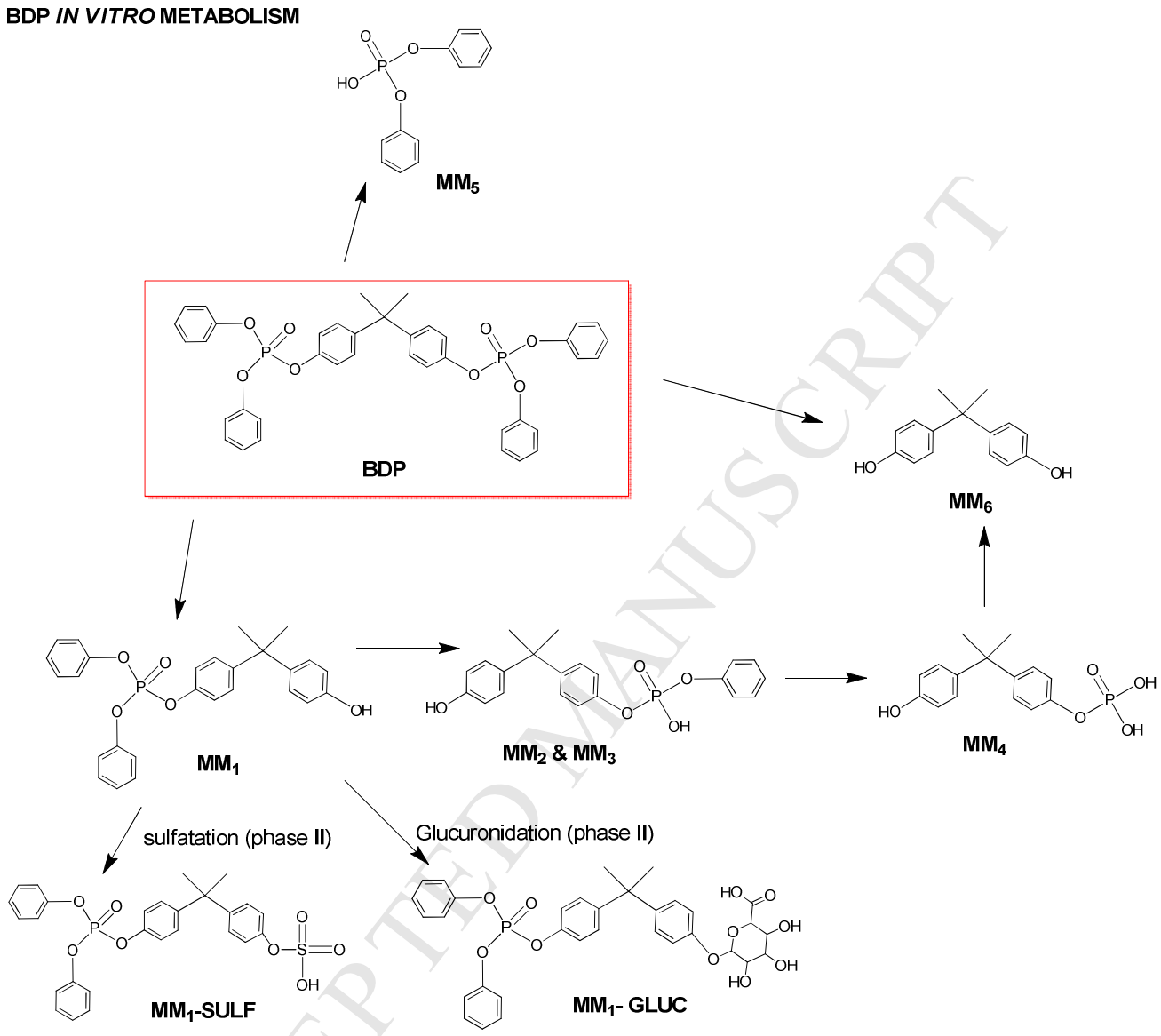

517 **Figure 4**. Formation of BDP phase I metabolite MM1 by seven rCYPs expressed in human
518 liver.

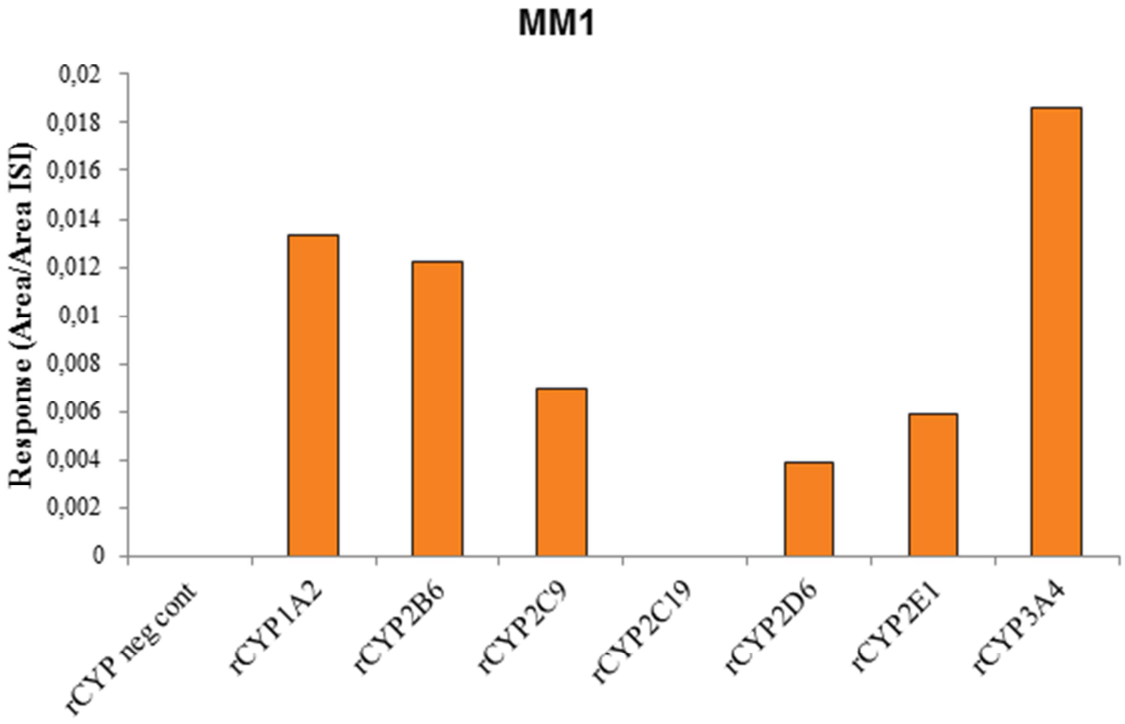

519

Highlights

- V6 forms hydroxylated and hydrolytic phase I metabolites by CYPs and PONs
- BDP forms hydrolytic and O-dealkylated phase I metabolites by PONs
- Only few glucuronidated and sulfated phase II metabolites were produced
- rCYP1A2 was responsible for the exclusive formation of two metabolites of V6
- CYPs are important in the metabolism of V6
- PONs have a predominant role in the *in vitro* metabolism of RDP